ACS chemical biology

Articles

pubs.acs.org/acschemicalbiology

# Phosphatase-Inert Glucosamine 6-Phosphate Mimics Serve as Actuators of the *glmS* Riboswitch

Xiang Fei,[†] Thomas Holmes,[‡] Julianna Diddle,[‡] Lauren Hintz,[‡] Dan Delaney,[‡] Alex Stock,[‡] Danielle Renner,[‡] Molly McDevitt,[‡] David B. Berkowitz,*[,†] and Juliane K. Soukup*[,‡]

[†]Department of Chemistry, University of Nebraska, Lincoln, Nebraska 68588, United States

[‡]Department of Chemistry, Creighton University, Omaha, Nebraska 68178, United States

Supporting Information

**ABSTRACT:** The *glmS* riboswitch is unique among gene-regulating riboswitches and catalytic RNAs. This is because its own metabolite, glucosamine-6-phosphate (GlcN6P), binds to the riboswitch and catalytically participates in the RNA self-cleavage reaction, thereby providing a novel negative feedback mechanism. Given that a number of pathogens harbor the *glmS* riboswitch, artificial actuators of this potential RNA target are of great interest. Structural/kinetic studies point to the 2-amino and 6-phosphate ester functionalities in GlcN6P as being crucial for this actuation. As a first step toward developing artificial actuators, we have synthesized a series of nine GlcN6P analogs bearing phosphatase-inert surrogates in place of the natural phosphate ester. Self-cleavage assays with the *Bacillus cereus glmS* riboswitch give a broad SAR. Two analogs display significant activity, namely, the 6-deoxy-6-phosphonomethyl analog (**5**) and the 6-*O*-malonyl ether (**13**). Kinetic profiles show a 22-fold and a 27-fold higher catalytic efficiency, respectively, for these analogs vs glucosamine (GlcN). Given their nonhydrolyzable phosphate surrogate functionalities, these analogs are arguably the most robust artificial *glmS* riboswitch actuators yet reported. Interestingly, the malonyl ether (**13**, extra O atom) is much more effective than the simple malonate (**17**), and the "sterically true" phosphonate (**5**) is far superior to the chain-truncated (**7**) or chain-extended (**11**) analogs, suggesting that positioning via Mg coordination is important for activity. Docking results are consistent with this view. Indeed, the viability of the phosphonate and 6-O-malonyl ether mimics of GlcN6P points to a potential new strategy for artificial actuation of the *glmS* riboswitch in a biological setting, wherein phosphatase-resistance is paramount.

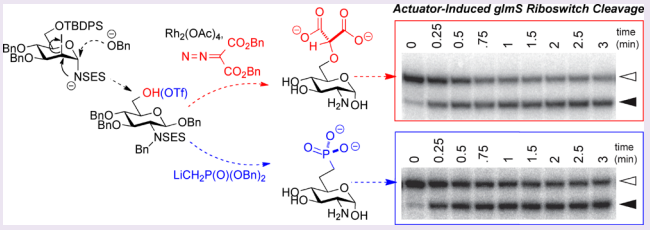


Riboswitches are found in noncoding regions of mRNAs, and gene expression is modulated when a metabolite binds directly to the RNA. Many riboswitches, once liganded, repress expression of associated or adjacent genes involved in the synthesis of the metabolite, providing an efficient feedback mechanism of genetic control.[1,2] The *glmS* riboswitch resides upstream of the *glmS* gene in *B. subtilis* and in a number of other Gram-positive bacteria.[3] It is an essential gene that encodes for the GlmS enzyme, glucosamine 6-phosphate synthase, which uses fructose-6-phosphate (Fru6P) and glutamine to generate glucosamine-6-phosphate (GlcN6P).[4] This reaction is the first committed step in the pathway that produces UDP-N-acetylglucosamine, key for bacterial cell wall biosynthesis.[4,5] The *glmS* riboswitch is found in high profile bacterial targets, including *B. anthracis*, *Clostridium difficile*, and *Staphylococcus aureus*, motivating efforts to develop artificial actuators.[6−8] Indeed, structure−activity relationship (SAR) studies of other riboswitches and how they interact with their cognate metabolites have enabled rational design of artificial agonists and ultimately antibiotics.[8,9]

The *glmS* riboswitch consists of four paired regions P1−P4 that exhibit a high level of sequence conservation, particularly within the catalytic core where nucleotide identities are >95% conserved (Figure 1).[3,10] The *glmS* riboswitch is mechanistically unique as it is the only known riboswitch for which catalytic activity provides the basis of genetic regulation, and it is the only known ribozyme that depends upon a "coenzyme" or actuator, namely its metabolite GlcN6P, for self-cleavage.[11,12] The *glmS* riboswitch/ribozyme selectively binds GlcN6P, thereby accelerating the cleavage reaction by at least 6 orders of magnitude.[3,12] This results in the release of a large downstream fragment, including the coding region of the mRNA that is degraded by RNase J1.[13] In the presence of GlcN6P but not UDP-N-acetylglucosamine, the final product of this pathway, the intracellular concentration of the GlmS enzyme, is decreased, but expression is not completely inhibited.[4]

The *glmS* riboswitch self-cleavage mechanism most consistent with experimental evidence to date is illustrated in Figure 2.[12,14−20] Whereas early on it had been postulated that G33 could serve as the general base needed for 2′-OH deprotonation at the A1 position,[17] discrepancies between the p$K_a$ of the cleavage reaction and both the calculated[21] and the measured microscopic[22] p$K_a$ of G33 called this into question. In

**Received:** June 8, 2014
**Accepted:** September 25, 2014
**Published:** September 25, 2014

  

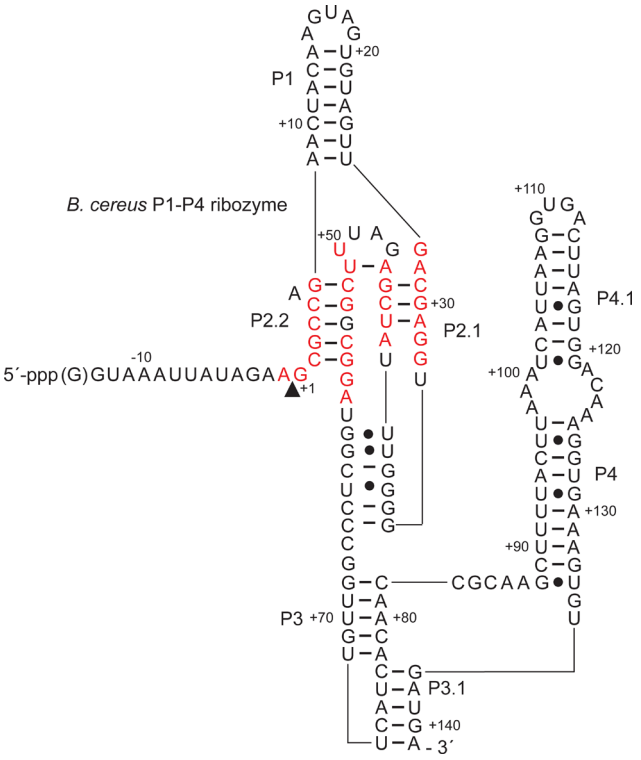


**Figure 1.** Secondary structure of the *Bacillus cereus glmS* riboswitch/ribozyme. The highly conserved core sequence of the *glmS* ribozyme is shown in red (P2.1 and P2.2), while requisite structural elements (P1 and P2) and peripheral structural elements (P3–P4) are also displayed with nucleotide detail. The arrowhead denotes the site of self-cleavage.

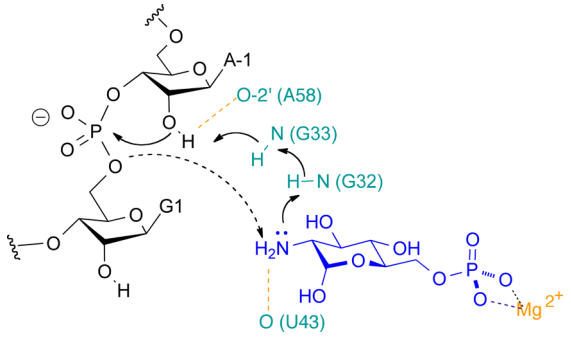


**Figure 2.** Illustration of the dual general base/acid mechanism for GlcN6P-promoted strand scission in the *glmS* ribozyme. GlcN6P is proposed to promote 2′,3′-cyclic phosphodiester formation by completing a circuit of proton transfer events that includes (indirect) deprotonation of the nucleophilic 2′-OH of the A-1 riboside and protonation of the 5′-O leaving group. Other active site bases that have been implicated in proton transfer or H-bonding roles here include the O2′ of A58, N1 of G33, N1 of G32, and O4 of U43.

fact, it has been demonstrated that *glmS* self-cleavage is dependent upon the p$K_a$ of the amine functionality of GlcN6P and other actuators,[12] with a Bronsted $\beta$ value of 0.7 having been observed in a recent study, suggesting that the general base role resides in the GlcN6P ligand itself.[23] GlcN6P analogs that lack the amine functionality do not support *glmS* self-cleavage; those with elevated amine p$K_a$ values support self-cleavage activity at elevated reaction p$K_a$ values,[12] and those that remove the N lone pair via quaternization or sequestration through amide protection are also ineffective.[24]

The picture that has emerged is one in which the 2-amino group of GlcN6P serves as both a general base and a general acid, a mechanistic postulate that is well precedented in both related protein[25,26] and nucleic acid chemistry.[27,28] This proposal aligns nicely with Raman difference crystallography studies[29] and computational simulations,[30] indicating that upon riboswitch binding, the p$K_a$ of the GlcN6P amino group is lowered to align with the optimal reaction p$K_a$.

Beyond this, specific sugar hydroxyl groups also are advantageous for binding/catalysis,[12,15−18,20,24,31] with the 4-hydroxyl group serving as a hydrogen-bond donor. Interestingly, a carba-sugar analog of GlcN6P has been reported to promote *glmS* ribozyme self-cleavage with activity similar to that of the natural metabolite, suggesting that the ring oxygen is not essential.[31,32] Finally, the riboswitch selectively binds to the $\alpha$-anomer of GlcN6P, pointing to possible involvement of the anomeric hydroxyl in binding and/or catalysis.[33]

In addition to the structural constraints articulated above, available X-ray crystallographic structures suggest that the phosphate ester functionality is important for positioning the GlcN6P actuator in the riboswitch active site via chelation to $Mg^{2+}$. Given the susceptibility of phosphate esters to cleavage by digestive phosphatases, it was a principal goal of this study to develop riboswitch actuators that are phosphatase-inert. The simplest design might be to replace the bridging phosphate monoester oxygen with a carbon, to generate phosphonate analogs.

There is currently great interest in naturally occurring phosphonates, as antibiotics,[34] including the widely used fosfomycin,[35,36] a PEP analog that inactivates UDP-GlcNAc-3-enolpyruvyl transferase (MurA), a critical enzyme in bacterial cell wall biosynthesis. More recently, fosmidomycin has shown promise as a potential antituberculosis lead compound, as it potently inhibits DXR in the committed step for the nonmevalonate isoprenoid biosynthetic pathway.[37] Indeed, Metcalf and co-workers have dubbed this "an underexplored family of secondary metabolites."[38]

The Berkowitz group has a longstanding interest in the synthesis of unnatural phosphonates[39−45] and in their use to probe active sites[46] and glycoprotein receptor binding pockets,[47,48] for example. Therefore, we initially set about to construct a set of phosphonate mimics of GlcN6P as potential artificial actuators of the *glmS* riboswitch.

## RESULTS AND DISCUSSION

**Design and Synthesis of GlcN6P Analogs.** Synthetically, the key strategy undertaken was to develop a synthetic route into a viable glucosamine-6-*O*-triflate, for installation of various phosphate surrogate functionalities. In earlier work, we had established the utility of sugar triflate displacement with C-nucleophiles in general,[49] and toward sugar phosphonates in particular.[42−46,50] However, prior to this work, triflates derived from amino-sugars had not been synthesized or examined for displacement with this chemistry. A significant challenge was to install an amino protecting group (PG) that would be amenable to primary sugar triflate preparation. Initial forays into N-acetyl protection met with little success at the triflate installation stage. On the other hand, more strongly electron-withdrawing N-sulfonyl PGs proved successful, with the (2′-trimethylsilyl)-ethanesulfonyl (SES) PG being optimal.

The synthetic route begins with the glucal **1** and introduces the 2-amino functionality via glycal iodo-sulfonamidination (Figure 3). Then the amino group "rolls over" from the 1- to

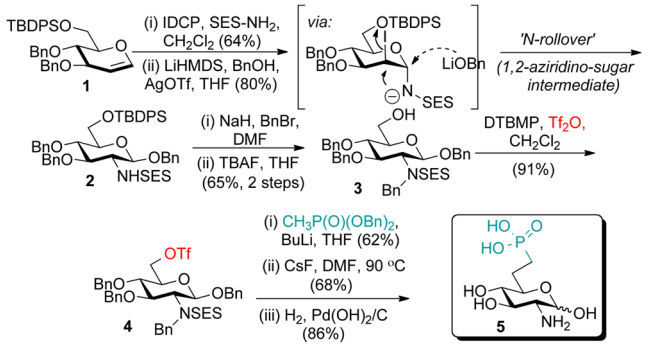


**Figure 3.** Sulfonamido-glycosylation/N-rollover entry to SES-protected glucosamino-triflate **4** leading to GlcN6P phosphonate analog **5**; IDCP = iodonium di(*sym*-collidine) perchlorate.

the 2-position, via a presumed N-sulfonyl aziridine intermediate.[51,52] With further protection of the nitrogen and removal of 6-O-silyl PG, the free alcohol **3** was prepared and stored in large quantity. The reaction between **3** and triflic anhydride under basic conditions gave the glucosamine 6-O-triflate **4** expeditiously (91% yield). Direct displacement with lithiomethyl dibenzyl phosphonate[53] proceeded smoothly and was followed by SES deprotection and subsequent catalytic hydrogenation to afford the phosphonate **5**, the targeted GlcN6P surrogate, for the first time.

In addition, we set out to explore tether length in such phosphonate-based analogs (Figure 4). $S_N2$ substitution of the

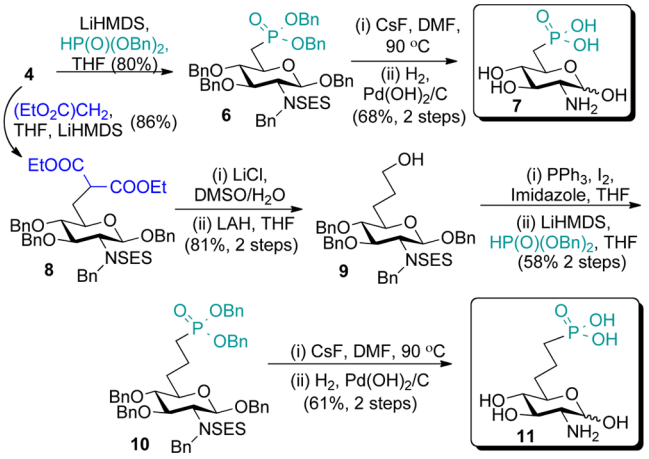


**Figure 4.** Triflate displacement route into the "truncated" and "elongated" analogs of the parent GlcN6P-phosphonate mimic.

key intermediate triflate **4** by dibenzyl phosphite anion afforded compound **6** in 80% yield. Following the standard deprotection method, "truncated" phosphonate **7** was synthesized. Triflate displacement by a malonate anion followed by a decarboxylation/reduction sequence built the "elongated" alcohol **9**. However, the extended triflate was unstable even at low temperature (−40 °C). Thus, an iodide intermediate was instead employed. Displacement with a phosphite anion and then sequential N-SES and global benzyl deprotection provided compound **11** as an "elongated" phosphonate analog.

Motivated by recent studies on a malonate-based analog that binds to a sugar phosphate-binding site in phosphomannose isomerase,[54] we next targeted three carboxylate-bearing GlcN6P surrogates. One of these, namely the malonyl ether **13**, was constructed by Rh(II)-mediated O−H insertion of the carbenoid species derived from dibenzyl diazomalonate (Figure 5). The dicarboxylic acid derivative **17** and the monocarboxylic

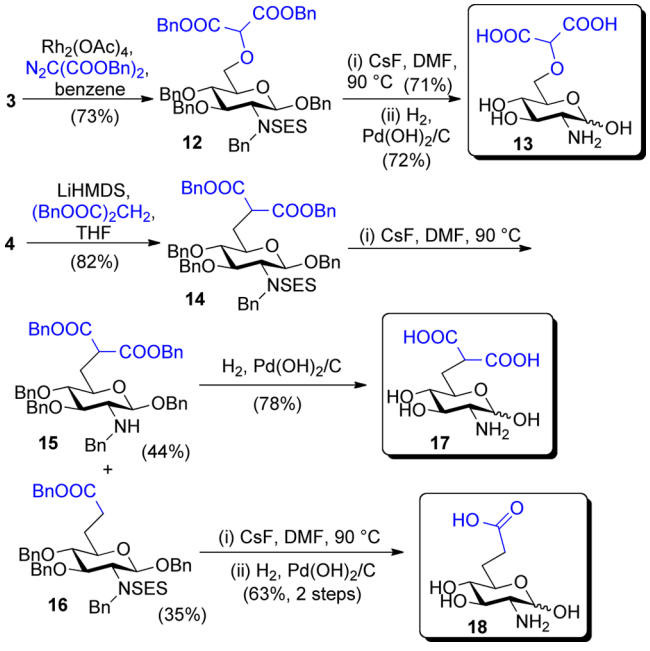


**Figure 5.** Synthesis of GlcN6P analogs with mono- and bis-carboxylate-based phosphate surrogates.

acid derivative **18**, in turn, could be accessed from intermediate **14**, which was efficiently formed in the reaction of triflate **4** and lithiodibenzyl malonate.

The GlcN6P-like phosphoramide was next targeted as the aza-analog of the parent phosphate monoester. The common precursor triflate **4** was displaced by azide in 89% yield. Cleavage of the N-sulfonyl linkage with nucleophilic fluoride and then Staudinger reduction conveniently produced compound **20**. The primary amine was then reacted with dibenzyl chlorophosphate to install the phosphoramide. Global debenzylation gave phosphoramide analog **22** (Figure 6).

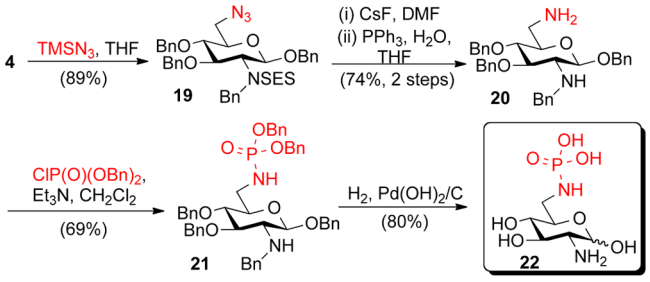


**Figure 6.** Construction of the phosphoramide GlcN6P analog.

Because of the key role postulated for the 2-amino group in catalysis, N-methylation was next explored.[24] Thus, silyl ether **2** was methylated and deprotected with TBAF. Following triflate displacement, deprotection of the SES amide and global benzylation afforded N-monomethylated phosphonate **27** (Figure 7). The SES-deprotected compound **25** could be further methylated with methyl iodide, to yield the N,N-dimethyl analog **28**, after deprotection.


dx.doi.org/10.1021/cb500458f | ACS Chem. Biol. 2014, 9, 2875−2882

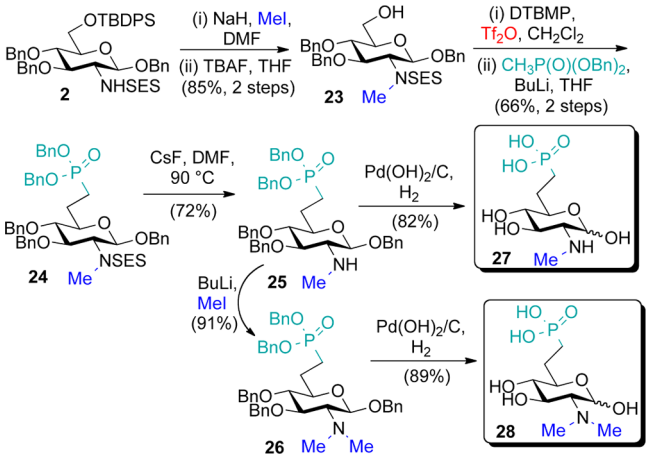


**Figure 7.** Synthesis of the N-mono- and N,N-dimethylamino derivatives of the parent phosphonate.

**Self-Cleavage Assays with the *glmS* Riboswitch.** The *Bacillus cereus glmS* ribozyme was utilized in self-cleavage kinetic assays performed in the presence of various synthesized GlcN6P analogs. Nine analogs were tested for their ability to support *glmS* self-cleavage (Figure 8). Seven of the nine analogs contain an unmodified amine functionality. The remaining two analogs combine the "sterically true" phosphonate ester with N-methylated amino groups. Mono- or dimethylation of the amine still retains the lone pair on nitrogen, which would, in principle, still allow the amine to function as a general base/acid.

Cleavage assays and data are presented in Figure 8 and Table 1, as well as in the SI. Of the nine analogs tested, five exhibited significant self-cleavage rates ($k_{obs}$), namely, the sterically true phosphonate (**5**) and its N-methyl (**27**) and N,N-dimethyl (**28**) congeners, as well as the malonyl ether (**13**) and the phosphoramide (**22**). While GlcN6P is the natural actuator/ligand for the *glmS* riboswitch, the self-cleavage rate is difficult to measure accurately (see range given in Table 1), with reported values for the $k_{obs}$(GlcN6P)/$k_{obs}$(GlcN) ratio ranging from 37:1[12] to 143:1.[23] Therefore, for experimental benchmarking, we have chosen to compare our results to the ligand analog GlcN. The observed pseudo-first-order rate constants ($k_{obs}$) for riboswitch cleavage with the artificial actuators at pH 7.3 are collected in the table.

As can be seen from the primary data (see SI), the other four analogs, namely the chain-truncated phosphonate (**7**), the chain-elongated phosphonate (**11**), the simple malonate (**17**), and the monocarboxylate (**18**), show only very modest induction of *glmS* riboswitch self-cleavage (Note: Owing to limited quantities of material, compounds **11** and **18** were tested at 1 mM concentrations, rather than the 10 mM concentrations used for the other analogs).

Follow-up kinetic assays were conducted on the five most active analogs, the sterically true phosphonate (**5**) and its N-methyl (**27**) and N,N-dimethyl (**28**) congeners, as well as the malonyl ether (**13**) and the phosphoramide (**22**). These experiments were undertaken to estimate pseudo-second-order rate constants (i.e., $k_{cat}/K_m$) at subsaturating cofactor concentrations, according to the approach of Fedor and Viladoms.[23] Pleasingly, the "sterically true" phosphonate analog (**5**) and the 6-*O*-malonyl ether (**13**) exhibited the greatest catalytic efficiency, 22-fold and 27-fold more reactive than glucosamine, respectively (Table 1).

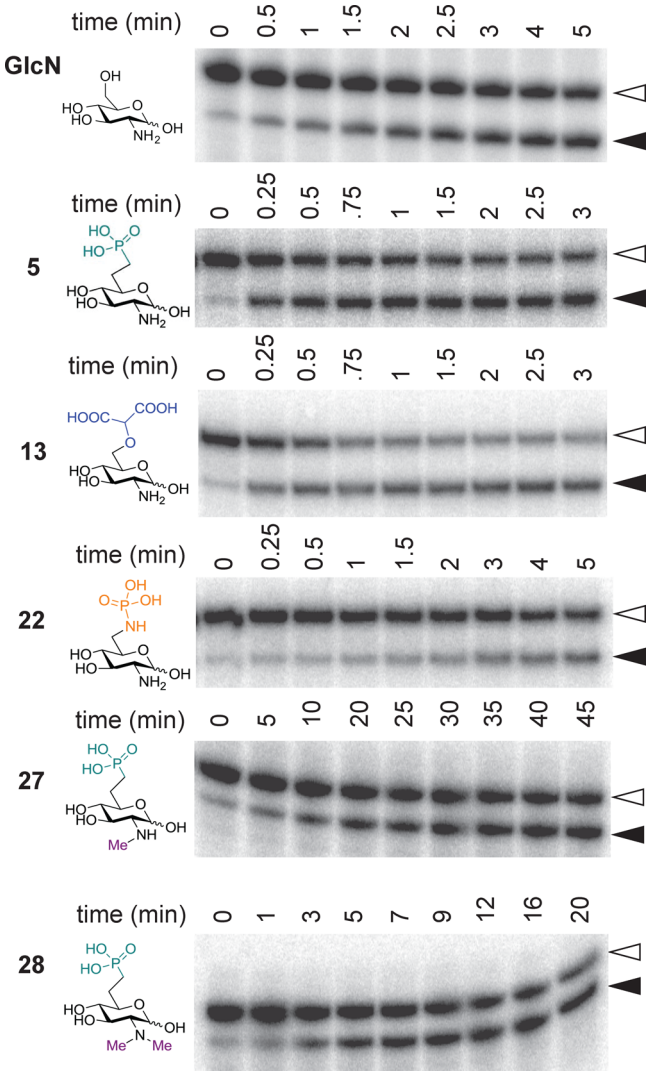


**Figure 8.** GlcN6P analog-actuated *glmS* ribozyme self-cleavage. Shown are products of reactions incubated for varying times in the presence of 10 mM analog. Bands correspond to the ribozyme (open arrowhead) and its 3′-cleavage product (filled arrowhead). Note: Data for the less active analogs is in the SI.

**Table 1. Kinetic Parameters for *glmS* Self-Cleaving Ribozyme**

| actuator | $k_{obs}$ ($min^{-1}$)[a] | $k_{cat}/K_m$ ($mM^{-1}min^{-1}$)[b] | RCE[c] |
|---|---|---|---|
| **5** | 0.924 ± 0.10 | 0.394 | 22.1 |
| **13** | 1.01 ± 0.21 | 0.488 | 27.4 |
| **17** | 0.00579 ± 0.00015 | 0.0016 | 0.0898 |
| **22** | 0.101 ± 0.013 | 0.0101 | 0.567 |
| **27** | 0.027 ± 0.011 | 0.0035 | 0.197 |
| **28** | 0.0423 ± 0.010 | 0.0100 | 0.562 |
| **GlcN** | 0.174 ± 0.025 | 0.0178 | 1.00 |
| **GlcN6P** | 1.1−100[12,23] | ~98[23] | 5510 |

[a]10 mM actuator, pH 7.3, 25 °C; rates are ± standard deviation. [b]1.0−0.01 mM actuator, pH 7.3, 25 °C. [c]Relative Catalytic Efficiency (RCE) = $k_{cat}/K_m$ relative to GlcN.

These results provide strong support for the notion that the phosphate is critical to GlcN6P positioning in the riboswitch "active site." This is seen in the phosphonate series, in which


dx.doi.org/10.1021/cb500458f | ACS Chem. Biol. 2014, 9, 2875−2882

only the analog (**5**) possessing a single methylene ($CH_2$) unit in place of the bridging phosphate oxygen is effective. Deletion of this methylene (in **7**) or insertion of an additional methylene (in **11**) all but abolishes this activity. In addition to this apparent positioning constraint, a dianionic end group also appears to be advantageous. This can be seen in the carboxylate mimic series, wherein the monocarboxylate (**18**) is nearly inactive.

Further modifications to the best phosphonate analog (**5**), namely N-mono- and dimethylation, did not lead to improved activity. The measured $pK_{a2}$ for the monomethylated analog (**27**) is 8.2, whereas the $pK_{a2}$ for the dimethylated analog (**28**) is 7.8. So, based upon acid−base chemistry considerations alone, one might predict that the latter analog would be the superior analog. Indeed, while **28** does outperform **27**, given that **5** displays a nearly 40-fold better $k_{cat}/K_m$, relative to both **27** and **28**, it would appear that in this series, deleterious sterics are the dominant factor.

We set about to examine the binding of the most promising analogs more closely via molecular docking. There are currently six published X-ray crystal structures of the *glmS* riboswitch precleavage complex with GlcN6P bound, four from *Thermoanaerobacter tengcongensis* (2Z74, 2Z75, 3B4B, 3B4C)[15,17,18] and two from *Bacillus anthracis* [3G8T (G33A, 2NZ4 (2′OMe-A-1))].[16,20] The latter structure was chosen as the *B. anthracis* riboswitch displays 98% identity with the *B. cereus* riboswitch employed in the cleavage assays in this work. As can be seen in Figure 9, deletion of the bound GlcN6P,

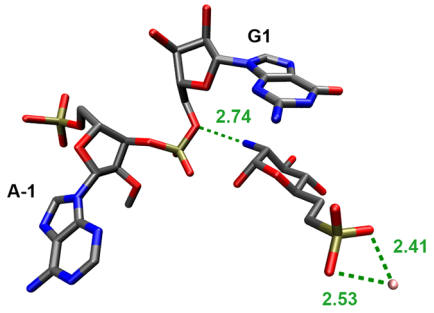


**Figure 9.** Projected orientation of phosphonate analog **5** when bound to *glmS* riboswitch; docked to *glmS* structure **2NZ4** (*Bacillus anthracis*).

followed by molecular docking (Autodock 4-see SI for details) of the dianionic form of phosphonate **5** supports a model in which $Mg^{2+}$-coordination projects the 2-amino group appropriately for its putative general acid/base function in the cleavage reaction.

To better assess ligand charge, titrations for the most interesting analogs were carried out, and the results are tabulated in the SI. Of potential significance, the second $pK_a$ of phosphonate analog **5** was determined to be ∼7.4 from titration curves (SI: Figure S2A). Therefore, under the cleavage assay conditions (pH 7.3), only ∼50% of the phosphonate moiety is dianionic, although modeling suggests that this form is required for optimal binding through magnesium ion chelation. Therefore, the diminished activity of **5** relative to the native GlcN6P ligand ($pK_{a2}$ ∼ 6.2)[12] and to the malonyl ether (**13**) may be at least in part due to the elevated second $pK_a$ of phosphonate.

Interestingly, the simple malonate analog, **17**, is ∼300-fold less active than the malonyl ether analog **13**. Titration of these 1,3-dicarboxylic acids indicates that $pK_{a2}$ of the malonate analog (**17**) is 5.3 and that of the malonyl ether (**13**) is 3.9 (SI: Figure S2). Therefore, both of these bis-carboxylates are in their dianionic forms under the conditions of the assay. Given this, each analog was docked to the *glmS* riboswitch in dianionic form. The results are striking (Figure 10). The malonyl ether

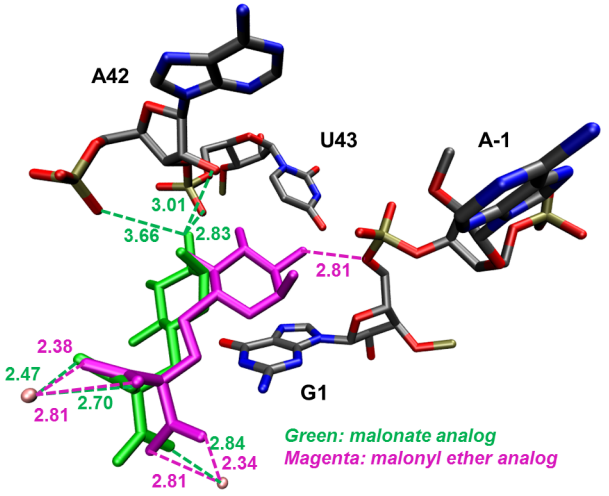


**Figure 10.** Overlay of docked structures of malonate and malonyl ether analogs in the active site. Green represents malonate analog; magenta represents malonyl ether analog. The carboxylates of the malonyl ether bind tightly with two $Mg^{2+}$ ions with the amino group poised to protonate the leaving oxygen atom. In the malonate analog, coordination to two $Mg^{2+}$ ions is also predicted. However, for this analog, the amino group docks near the A42−U43 phosphodiester, instead of the scissile A-1-G1 phosphodiester, consistent with the weak actuator activity of compound **17**.

analog is well positioned in the active site. *However, in contrast to the native GlcN6P ligand or its phosphonate analog* **5**, *the bis-carboxylate moiety appears to permit coordination to two magnesium ions in the active site* (Figure 10). A similar bis-chelation motif is observed for the docked malonate (**17**) as well. However, for the latter ligand, docking suggests that the 2-amino group is improperly positioned for catalysis, interacting with the A42−U43 phosphodiester bond rather than with the susceptible phosphodiester linkage between A-1 and G1. Structural biology studies (e.g., cocrystallization) may be able to shed further light on this molecular-docking-based model for malonyl ether/malonate binding to the riboswitch in the future (Note: In response to a reviewer suggestion, a preliminary screen of self-cleavage rate vs $Mg^{2+}$ concentration was carried out with the P1−P4 construct of the *glmS* riboswitch and indicates that for both GlcN and GlcN6P, across a range of 1−100 mM $Mg^{2+}$, reaction rates are fairly constant, whereas the rate of the reaction with the malonyl ether (**13**) from 1 to 10 mM $Mg^{2+}$ increases 4.5-fold and then remains fairly constant from 10 to 100 mM).

In examining the literature on malonate-type surrogates for biological phosphates, one certainly finds cases in which simple malonates make for good analogs, in sharp contrast with our findings here, e.g., the aforementioned malonate analog of M6P (phosphomannose isomerase).[54] Indeed, in one head-to-head case carefully examined by Frost and co-workers, the malonate substrate analog displayed an order of magnitude superior activity to its malonyl ether counterpart in the inhibition of 3-dehydroquinate synthase.[55] Moreover, we previously saw a

similar preference for simple malonates over malonyl ether mimics of M6P in binding to the M6P-insulin-like growth factor II receptor.[48]

On the other hand, perhaps the best case of a particularly active malonyl ether phosphate mimic described heretofore was in a classic study by Sikorski et al. at Monsanto toward the development of novel EPSP synthase inhibitors.[56] However, this may be the first indication of the potential advantage of a malonyl ether in bis-carboxylate positioning for metal ion coordination, indeed possibly for bis-Mg coordination.

Taken together, the results of this study suggest that both the malonyl ether (**13**) and the sterically true phosphonate (**5**) mimics of GlcN6P are promising starting points for the development of phosphatase-resistant artificial actuators for the *glmS* riboswitch as is critical for *in vivo* application. We note that these actuators are only ∼1/7 as active as the natural ligand GlcN6P, and therefore there is potential for improvement. Future studies will be guided by the observations reported herein and will build upon these two promising lead platforms.

## METHODS

**Synthesis of GlcN6P Analogs.** The construction of the phosphonate analogs exploited the triflate displacement chemistry previously reported[53,57] where possible. A detailed description of the synthesis of all nine analogs and spectral data for each intermediate can be found in the Supporting Information.

**Preparation of RNA.** Templates for transcription were prepared by primer extension and PCR amplification using synthetic DNA corresponding to ribozyme sequence. Ribozymes were prepared by *in vitro* transcription using T7 RNA polymerase and $^{32}$P-labeled by incorporation of [$\alpha$-$^{32}$P]-UTP. Transcription products were separated by denaturing 10% polyacrylamide gel electrophoresis (PAGE), and ribozymes were eluted in solution containing 50 mM HEPES (pH 7.3 at 22 °C) and 200 mM NaCl, precipitated with ethanol, and redissolved in water.[12]

**Self-Cleavage Assay.** Ribozyme reactions were performed as previously described.[12,23] Briefly, reactions contained a ligand analog as indicated and were performed under standard conditions consisting of incubation at 22 °C in solution containing 50 mM HEPES pH 7.3. A saturating concentration of $MgCl_2$ was used in order to avoid a slow folding step and to allow for the formation of native *glmS* RNA structure.[20,58] The [$\alpha$-$^{32}$P]-UTP-labeled *glmS* ribozyme (<250 nM) was prefolded in 50 mM HEPES pH 7.5, 0.1 mM EDTA, and 50 mM $MgCl_2$ at 22 °C. Reactions were started by adding coenzyme at varying concentrations (10 mM−10 $\mu$M final concentration) in 50 mM HEPES pH 7.3 buffer. Reactions were terminated by the addition of a gel loading dye containing 10 M urea, 50 mM EDTA, 0.1% bromophenol blue, and 0.1% xylene cyanol. Products were separated by denaturing 10% PAGE and analyzed using a PhosphorImager and IMAGEQUANT software (Molecular Dynamics). $k_{obs}$ values for self-cleavage were derived by plotting the natural logarithm of the fraction of uncleaved ribozyme versus time and establishing the negative slope of the resulting line. Stated values represent the average of at least three replicate assays. First order cleavage rate constants were obtained at different concentrations of coenzyme in the linear range of a Michaelis−Menten plot (ligand concentration ∼20% of apparent $K_m$ value) and were fit by linear regression to obtain apparent second-order rate constants $k_{cat}/K_m$.[23]

## ASSOCIATED CONTENT

### Supporting Information

Details of the synthesis of all compounds, of analog titration, biological assays and molecular docking are available. This material is available free of charge via the Internet at http://pubs.acs.org.

## AUTHOR INFORMATION


### Corresponding Authors

*E-mail: dberkowitz1@unl.edu.
*E-mail: jksoukup@creighton.edu.


### Notes

The authors declare no competing financial interest.

## ACKNOWLEDGMENTS

The authors wish to thank the National Institutes of Health (GM-R15M083641) for support of this collaboration. The Soukup laboratory thanks M. and K. Delaney for their generous donation to riboswitch research. Additional support to J.K.S. and A.S. came from grants from the National Center for Research Resources (5P20RR016469) and the National Institute for General Medical Science (5P20GM103427), to L.H. from the Dr. R.M. and T.K. Ferlic Summer Research Scholarship Program, to A.S. as a Goldwater Scholar, and to J.K.S. and D.R. from the Clare Boothe Luce Women in Science Program, funded by the Luce Foundation. This research was facilitated by the IR/D (Individual Research and Development) program associated with D.B.B.'s appointment at the NSF. The authors thank the National Institutes of Health (SIG-1-510-RR-06307)/NSF (CHE-0091975, MRI0079750) (UN NMR) and National Institutes of Health (RR016544) (UN facilities).

## REFERENCES


(1) Mandal, M., and Breaker, R. R. (2004) Gene regulation by riboswitches. *Nat. Rev. Mol. Cell. Biol. 5*, 451−463.

(2) Serganov, A., and Nudler, E. (2013) A Decade of Riboswitches. *Cell 152*, 17−24.

(3) Winkler, W. C., Nahvi, A., Roth, A., Collins, J. A., and Breaker, R. R. (2004) Control of gene expression by a natural metabolite-responsive ribozyme. *Nature 428*, 281−286.

(4) Milewski, S. (2002) Glucosamine-6-phosphate synthase: the multi-facets enzyme. *Biochim. Biophys. Acta 1597*, 173−192.

(5) Badet-Denisot, M. A., Rene, L., and Badet, B. (1993) Mechanistic investigations on glucosamine-6-phosphate synthase. *Bull. Soc. Chim. Fr. 130*, 249−255.

(6) Deigan, K. E., and Ferre-D'Amare, A. R. (2011) Riboswitches: discovery of drugs that target bacterial gene-regulatory RNAs. *Acc. Chem. Res. 44*, 1329−1338.

(7) Lunse, C. E., Schuller, A., and Mayer, G. (2014) The promise of riboswitches as potential antibacterial drug targets. *Int. J. Med. Microbiol. 304*, 79−92.

(8) Blount, K. F., and Breaker, R. R. (2006) Riboswitches as antibacterial drug targets. *Nat. Biotechnol. 24*, 1558−1564.

(9) Lea, C. R., and Piccirilli, J. A. (2006) "Turning on" riboswitches to their antibacterial potential. *Nat. Chem. Biol. 3*, 16−17.

(10) Barrick, J. E., Corbino, K. A., Winkler, W. C., Nahvi, A., Mandal, M., Collins, J., Lee, M., Roth, A., Sudarsan, N., Jona, I., Wickiser, J. K., and Breaker, R. R. (2004) New RNA motifs suggest an expanded scope for riboswitches in bacterial genetic control. *Proc. Natl. Acad. Sci. U. S. A. 101*, 6421−6426.

(11) Soukup, J. K. (2013) The structural and functional uniqueness of the *glmS* ribozyme. *Prog. Mol. Biol. Transl. 120*, 173−193.

(12) McCarthy, T. J., Plog, M. A., Floy, S. A., Jansen, J. A., Soukup, J. K., and Soukup, G. A. (2005) Ligand requirements for *glmS* ribozyme self-cleavage. *Chem. Biol. 12*, 1221−1226.

(13) Collins, J. A., Irnov, I., Baker, S., and Winkler, W. C. (2007) Mechanism of mRNA destabilization by the *glmS* ribozyme. *Genes Dev. 21*, 3356−3368.

(14) Jansen, J. A., McCarthy, T. J., Soukup, G. A., and Soukup, J. K. (2006) Backbone and nucleobase contacts to glucosamine-6-phosphate in the *glmS* ribozyme. *Nat. Struct. Mol. Biol. 13*, 517−523.

(15) Klein, D. J., and Ferre-D'Amare, A. R. (2006) Structural basis of *glmS* ribozyme activation by glucosamine-6-phosphate. *Science 313*, 1752−1756.
(16) Cochrane, J. C., Lipchock, S. V., and Strobel, S. A. (2007) Structural investigation of the *glmS* ribozyme bound to its catalytic cofactor. *Chem. Biol. 14*, 97−105.
(17) Klein, D. J., Been, M. D., and Ferre-D'Amare, A. R. (2007) Essential role of an active-site guanine in *glmS* ribozyme catalysis. *J. Am. Chem. Soc. 129*, 14858−14859.
(18) Klein, D. J., Wilkinson, S. R., Been, M. D., and Ferre-D'Amare, A. R. (2007) Requirement of helix P2.2 and nucleotide G1 for positioning the cleavage site and cofactor of the *glmS* ribozyme. *J. Mol. Biol. 373*, 178−189.
(19) Tinsley, R. A., Furchak, J. R. W., and Walter, N. G. (2007) Trans-acting *glmS* catalytic riboswitch: locked and loaded. *RNA 13*, 468−477.
(20) Cochrane, J. C., Lipchock, S. V., Smith, K. D., and Strobel, S. A. (2009) Structural and chemical basis for glucosamine 6-phosphate binding and activation of the *glmS* ribozyme. *Biochemistry 48*, 3239−3246.
(21) Banas, P., Walter, N. G., Sponer, J., and Otyepka, M. (2010) Protonation States of the Key Active Site Residues and Structural Dynamics of the *glmS* Riboswitch As Revealed by Molecular Dynamics. *J. Phys. Chem. B 114*, 8701−8712.
(22) Viladoms, J., Scott, L. G., and Fedor, M. J. (2011) An Active-Site Guanine Participates in *glmS* Ribozyme Catalysis in Its Protonated State. *J. Am. Chem. Soc. 133*, 18388−18396.
(23) Viladoms, J., and Fedor, M. J. (2012) The *glmS* ribozyme cofactor is a general acid-base catalyst. *J. Am. Chem. Soc. 134*, 19043−19049.
(24) Lim, J., Grove, B. C., Roth, A., and Breaker, R. R. (2006) Characteristics of ligand recognition by a *glmS* self-cleaving ribozyme. *Angew. Chem., Int. Ed. 45*, 6689−6693.
(25) Thompson, J. E., and Raines, R. T. (1994) Value of General Acid-Base Catalysis to Ribonuclease A. *J. Am. Chem. Soc. 116*, 5467−5468.
(26) Breslow, R., and Chapman, W. H., Jr. (1996) On the mechanism of action of ribonuclease A: relevance of enzymic studies with a p-nitrophenylphosphate ester and a thiophosphate ester. *Proc. Natl. Acad. Sci. U. S. A. 93*, 10018−10021.
(27) Bevilacqua, P. C., Brown, T. S., Nakano, S.-i., and Yajima, R. (2004) Catalytic roles for proton transfer and protonation in ribozymes. *Biopolymers 73*, 90−109.
(28) Kath-Schorr, S., Wilson, T. J., Li, N.-S., Lu, J., Piccirilli, J. A., and Lilley, D. M. J. (2012) General Acid-Base Catalysis Mediated by Nucleobases in the Hairpin Ribozyme. *J. Am. Chem. Soc. 134*, 16717−16724.
(29) Gong, B., Klein, D. J., Ferre-D'Amare, A. R., and Carey, P. R. (2011) The *glmS* Ribozyme Tunes the Catalytically Critical p$K_a$ of Its Coenzyme Glucosamine-6-phosphate. *J. Am. Chem. Soc. 133*, 14188−14191.
(30) Xin, Y., and Hamelberg, D. (2010) Deciphering the role of glucosamine-6-phosphate in the riboswitch action of *glmS* ribozyme. *RNA 16*, 2455−2463.
(31) Lünse, C. E., Schmidt, M. S., Wittmann, V., and Mayer, G. (2011) Carba-sugars activate the *glmS*-riboswitch of *Staphylococcus aureus*. *ACS Chem. Biol. 6*, 675−678.
(32) Wang, G. N., Lau, P. S., Li, Y. F., and Ye, X. S. (2012) Synthesis and evaluation of glucosamine-6-phosphate analogues as activators of *glmS* riboswitch. *Tetrahedron 68*, 9405−9412.
(33) Davis, J. H., Dunican, B. F., and Strobel, S. A. (2011) *glmS* riboswitch binding to the glucosamine-6-phosphate $\alpha$-anomer shifts the p$K_a$ toward neutrality. *Biochemistry 50*, 7236−7242.
(34) Metcalf, W. W., and van der Donk, W. A. (2009) Biosynthesis of phosphonic and phosphinic acid natural products. *Annu. Rev. Biochem. 78*, 65−94.
(35) Michalopoulos, A. S., Livaditis, I. G., and Gougoutas, V. (2011) The revival of fosfomycin. *Int. J. Infect. Dis. 15*, e732−e739.
(36) Chang, W.-c., Dey, M., Liu, P., Mansoorabadi, S. O., Moon, S.-J., Zhao, Z. K., Drennan, C. L., and Liu, H.-w. (2013) Mechanistic studies of an unprecedented enzyme-catalysed 1,2-phosphono-migration reaction. *Nature 496*, 114−118.
(37) Kholodar, S. A., Tombline, G., Liu, J., Tan, Z., Allen, C. L., Gulick, A. M., and Murkin, A. S. (2014) Alteration of the Flexible Loop in 1-Deoxy-D-xylulose-5-phosphate Reductoisomerase Boosts Enthalpy-Driven Inhibition by Fosmidomycin. *Biochemistry 53*, 3423−3431.
(38) Evans, B. S., Zhao, C., Gao, J., Evans, C. M., Ju, K.-S., Doroghazi, J. R., van der Donk, W. A., Kelleher, N. L., and Metcalf, W. W. (2013) Discovery of the Antibiotic Phosacetamycin via a New Mass Spectrometry-Based Method for Phosphonic Acid Detection. *ACS Chem. Biol. 8*, 908−913.
(39) Panigrahi, K., Nelson, D. L., and Berkowitz, D. B. (2012) Unleashing a "True" pSer-Mimic in the Cell. *Chem. Biol. 19*, 666−667.
(40) Panigrahi, K., Eggen, M., Maeng, J. H., Shen, Q. R., and Berkowitz, D. B. (2009) The alpha,alpha-Difluorinated Phosphonate L-pSer-Analogue: An Accessible Chemical Tool for Studying Kinase-Dependent Signal Transduction. *Chem. Biol. 16*, 928−936.
(41) Berkowitz, D. B., Bose, M., and Asher, N. G. (2001) A Convergent Triflate Displacement Approach to (alpha-Monofluoroalkyl)phosphonates. *Org. Lett. 3*, 2009−2012.
(42) Berkowitz, D. B., and Bose, M. (2001) (Alpha-monofluoroalkyl)phosphonates: a class of isoacidic and "tunable" mimics of biological phosphates. *J. Fluor. Chem. 112*, 13−33.
(43) Berkowitz, D. B., Bhuniya, D., and Peris, G. (1999) Facile installation of the phosphonate and (alpha,alpha-difluoromethyl)-phosphonate functionalities equipped with benzyl protection. *Tetrahedron Lett. 40*, 1869−1872.
(44) Berkowitz, D. B., Eggen, M., Shen, Q., and Shoemaker, R. K. (1996) Ready Access to Fluorinated Phosphonate Mimics of Secondary Phosphates. Synthesis of the (alpha,alpha-Difluoroalkyl)-phosphonate Analogs of L-Phosphoserine, L-Phosphoallothreonine, and L-Phosphothreonine. *J. Org. Chem. 61*, 4666−4675.
(45) Berkowitz, D. B., and Sloss, D. G. (1995) Diallyl (Lithiodifluoromethyl)phosphonate: A New Reagent for the Introduction of the (Difluoromethylene)phosphonate Functionality. *J. Org. Chem. 60*, 7047−7050.
(46) Berkowitz, D. B., Bose, M., Pfannenstiel, T. J., and Doukov, T. (2000) alpha-Fluorinated Phosphonates as Substrate Mimics for Glucose 6-Phosphate Dehydrogenase: the CHF Stereochemistry Matters. *J. Org. Chem. 65*, 4498−4508.
(47) Fei, X., Connelly, C. M., MacDonald, R. G., and Berkowitz, D. B. (2008) A set of phosphatase-inert "molecular rulers" to probe for bivalent mannose 6-phosphate ligand-receptor interactions. *Bioorg. Med. Chem. Lett. 18*, 3085−3089.
(48) Berkowitz, D. B., Maiti, G., Charette, B. D., Dreis, C. D., and MacDonald, R. G. (2004) Mono- and bivalent ligands bearing mannose 6-phosphate (M6P) surrogates: targeting the M6P/insulin-like growth factor II receptor. *Org. Lett. 6*, 4921−4924.
(49) Shen, Q. R., Sloss, D. G., and Berkowitz, D. B. (1994) Displacement of Sugar Triflates with C-Nucleophiles - D-Glucopyranose and D-Ribofuranose Chain Extension and Functionalization. *Synth. Commun. 24*, 1519−1530.
(50) Berkowitz, D. B., Eggen, M., Shen, Q., and Sloss, D. G. (1993) Synthesis of (alpha,alpha-Difluoroalkyl)Phosphonates by Displacement of Primary Triflates. *J. Org. Chem. 58*, 6174−6176.
(51) Griffith, D. A., and Danishefsky, S. J. (1990) Sulfonamidoglycosylation of glycals. A route to oligosaccharides with 2-aminohexose subunits. *J. Am. Chem. Soc. 112*, 5811−5819.
(52) Griffith, D. A., and Danishefsky, S. J. (1991) Total synthesis of allosamidin. An application of the sulfonamidoglycosylation of glycals. *J. Am. Chem. Soc. 113*, 5863−5864.
(53) Shen, Q. R., Sloss, D. G., and Berkowitz, D. B. (1994) Displacement of sugar triflates with C-Nucleophiles: D-glucopyranose and D-ribofuranose chain extension and functionalization. *Synth. Commun. 24*, 1519−1530.

(54) Gresh, N., de Courcy, B., Piquemal, J.-P., Foret, J., Courtiol-Legourd, S., and Salmon, L. (2011) Polarizable Water Networks in Ligand-Metalloprotein Recognition. Impact on the Relative Complexation Energies of Zn-Dependent Phosphomannose Isomerase with D-Mannose 6-Phosphate Surrogates. *J. Phys. Chem. B 115*, 8304−8316.
(55) Tian, F., Montchamp, J.-L., and Frost, J. W. (1996) Inhibitor Ionization as a Determinant of Binding to 3-Dehydroquinate Synthase. *J. Org. Chem. 61*, 7373−7381.
(56) Miller, M. J., Cleary, D. G., Ream, J. E., Snyder, K. R., and Sikorski, J. A. (1995) New EPSP synthase inhibitors: synthesis and evaluation of an aromatic tetrahedral intermediate mimic containing a 3-malonate ether as a 3-phosphate surrogate. *Bioorg. Med. Chem. 3*, 1685−1692.
(57) Berkowitz, D. B., Eggen, M., Shen, Q., and Sloss, D. G. (1993) Synthesis of (alpha,alpha-difluoroalkyl)phosphonates by displacement of primary triflates. *J. Org. Chem. 58*, 6174−6176.
(58) Brooks, K. M., and Hampel, K. J. (2009) A rate-limiting conformational step in the catalytic pathway of the *glmS* ribozyme. *Biochemistry 48*, 5669−5678.